Inducing host protection in pneumococcal sepsis by preactivation of the Ashwell-Morell receptor

Prabhjit K. Grewal[a,b], Peter V. Aziz[a,b], Satoshi Uchiyama[c], Gabriel R. Rubio[a,b], Ricardo D. Lardone[a,b], Dzung Le[d], Nissi M. Varki[d], Victor Nizet[c], and Jamey D. Marth[a,b,1]

[a]Center for Nanomedicine, University of California, Santa Barbara, CA 93106; [b]Sanford-Burnham Medical Research Institute, La Jolla, CA 92037; and [c]Department of Pediatrics, Skaggs School of Pharmacy and Pharmaceutical Sciences and [d]Department of Pathology, University of California, San Diego, La Jolla, CA 92093

Edited* by Kevin P. Campbell, University of Iowa Carver College of Medicine, Iowa City, IA, and approved October 21, 2013 (received for review July 23, 2013)

The endocytic Ashwell-Morell receptor (AMR) of hepatocytes detects pathogen remodeling of host glycoproteins by neuraminidase in the bloodstream and mitigates the lethal coagulopathy of sepsis. We have investigated the mechanism of host protection by the AMR during the onset of sepsis and in response to the desialylation of blood glycoproteins by the NanA neuraminidase of *Streptococcus pneumoniae*. We find that the AMR selects among potential glycoprotein ligands unmasked by microbial neuraminidase activity in pneumococcal sepsis to eliminate from blood circulation host factors that contribute to coagulation and thrombosis. This protection is attributable in large part to the rapid induction of a moderate thrombocytopenia by the AMR. We further show that neuraminidase activity in the blood can be manipulated to induce the clearance of AMR ligands including platelets, thereby preactivating a protective response in pneumococcal sepsis that moderates the severity of disseminated intravascular coagulation and enables host survival.

Pathogens in the host bloodstream often induce a hyperactive coagulation cascade that can progress to disseminated intravascular coagulation with severe thrombosis, organ failure, and death (1–3). With current limited understanding of pathogen–host interactions, sepsis remains a debilitating and deadly syndrome with few treatment options (4, 5). An unexpected protective host response that reduces coagulopathy during sepsis caused by *Streptococcus pneumoniae* (*SPN*) was recently discovered in studies of the endocytic Ashwell-Morell receptor (AMR) (6, 7). Host protection by the AMR is linked to the hydrolysis of sialic acids from blood glycoproteins by the neuraminidase A (NanA) of *SPN*. Sialic acids are posttranslational glycan modifications often attached to underlying galactose on many cell surface and secreted glycoproteins (8, 9).

Neuraminidases (aka sialidases) produced by microbial pathogens hydrolyze sialic acids on glycoproteins to establish infection and facilitate host colonization (10). For example, NanA remodels mucosal cell surface glycoproteins to promote bacterial colonization of the upper respiratory tract (11, 12) and contributes to pulmonary inflammation along with the development of *SPN* pneumonia (13, 14). However, the host has adapted to counteract the pathological effects of this *SPN* virulence factor by the clearance from blood circulation of host factors bearing AMR ligands that have been unmasked by NanA desialylation.

In this study we have identified multiple blood components that are removed from circulation by the AMR and have determined which of these are primarily responsible for diminishing the lethal coagulopathy of *SPN* sepsis. We have further used this information to develop and assess a prophylactic approach that preactivates AMR function in the early phases of sepsis to reduce the severity and lethality of the ensuing coagulopathy.

Results

Intravenous (i.v.) administration of three different purified microbial neuraminidases each effectively desialylated platelets and induced a rapid moderate thrombocytopenia in mice (Fig. 1 *A* and *B* and Fig. S1). At saturating doses of neuraminidase activity, circulating platelet levels were reduced by 70% within 2 h, with thrombocytopenia persisting for up to 72 h, before platelets rebounded to normal abundance coincident with restoration of cell surface sialic acids. Neuraminidase-induced unmasking of galactose was detected on multiple blood glycoproteins, whereas no significant alterations occurred in blood chemistry or in the abundance of blood cells and various inflammation markers (Figs. S2 and S3 and Table S1). In addition, neuraminidase did not alter the expression of multiple glycoproteins and receptors residing at the platelet plasma membrane (Fig. S4). All microbial neuraminidases analyzed produced similar outcomes in these and subsequent experiments detailed below.

Bleeding times were rapidly increased within 2 h of i.v. administration of neuraminidase and continued to be elevated for up to 96 h (Fig. 1*C*). In animals lacking the AMR, i.v. neuraminidase treatment desialylated circulating platelets, whereas no change occurred in platelet levels, and bleeding times remained normal (Fig. 1 *D* and *E*). Gp1bα is a highly sialylated platelet glycoprotein that has been reported to facilitate platelet ingestion by the AMR in hepatocyte culture (15). Upon exposure to neuraminidase, platelets lacking Gp1bα exhibited fewer unmasked galactose termini on their cell surface glycoproteins compared with WT platelets (Fig. 1*F*). Adoptive transfer studies revealed that the rate of neuraminidase-induced platelet clearance by the AMR was markedly reduced in the absence of Gp1bα (Fig. 1*G*); nevertheless, circulating platelets were reduced by 70% after 24 h (Fig. 1*H*). Therefore, Gp1bα is required to achieve

Significance

Sepsis occurs in the presence of a pathogen in the blood, often with increased blood clotting and inflammation that can cause severe tissue damage and organ failure leading to death. This article reports the mechanism of host protection mediated by the Ashwell-Morell receptor (AMR) of hepatocytes during sepsis caused by *Streptococcus pneumoniae*. The AMR protects the host primarily by diminishing the abundance of circulating platelets that have been remodeled by pathogen neuraminidase activity, thereby reducing the severity of coagulopathy, diminishing organ failure, and permitting host survival. The AMR is further selective in moderating circulating coagulation factors that are primarily prothrombotic. This study also presents an approach to preactivate AMR function early in sepsis to augment host protection and survival.

Author contributions: J.D.M. designed research; P.K.G., P.V.A., S.U., G.R.R., R.D.L., D.L., N.M.V., and V.N. performed research; P.K.G., P.V.A., S.U., G.R.R., R.D.L., D.L., N.M.V., V.N., and J.D.M. analyzed data; and V.N. and J.D.M. wrote the paper.

The authors declare no conflict of interest.

*This Direct Submission article had a prearranged editor.

[1]To whom correspondence should be addressed. E-mail: jmarth@sanfordburnham.org.

This article contains supporting information online at www.pnas.org/lookup/suppl/doi:10.1073/pnas.1313905110/-/DCSupplemental.

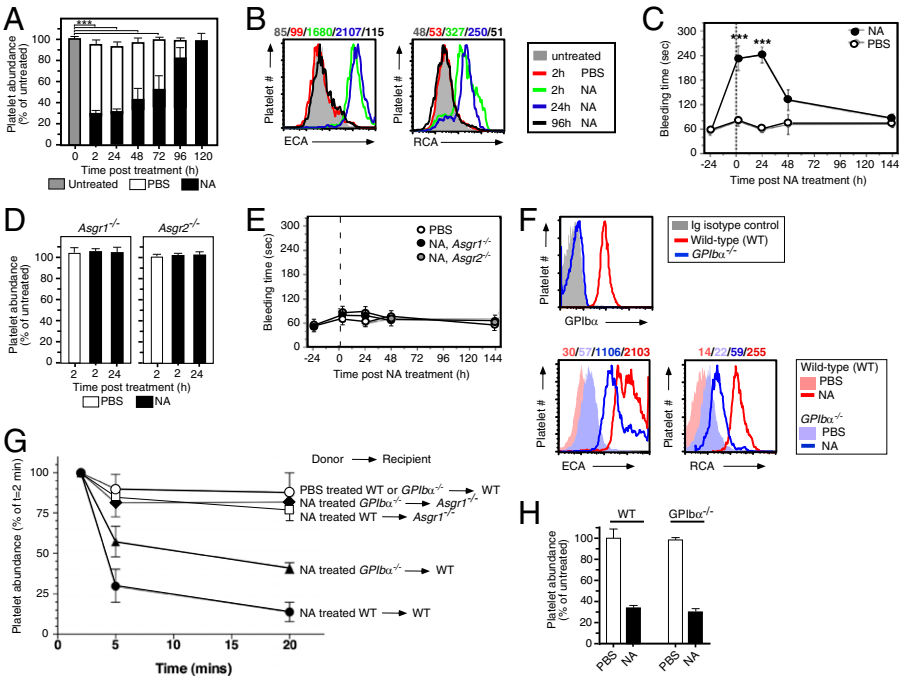

Fig. 1. Intravenous neuraminidase treatment in platelet desialylation and turnover, bleeding time increases, and Gp1bα-dependent platelet clearance involving AMR function. (*A*) Circulating platelet abundance, (*B*) *Erythrina cristagalli* lectin (ECA) and *Ricinus communis*-1 agglutinin (RCA-I) lectin binding at the platelet surface, and (*C*) bleeding times in response to a single i.v. administration of neuraminidase (NA) or PBS in WT mice. (*D*) Platelet abundance and (*E*) bleeding times among mice identically treated but lacking either Asgr1 or Asgr2 components of the AMR. (*F*) Gp1bα deficiency and neuraminidase-induced desialylation among platelets of indicated genotypes. (*G*) Circulating platelet clearance after platelet isolation, labeling, and transfer among mice of indicated donor and recipient genotypes. (*H*) Platelet abundance in WT or GP1bα-deficient mice 24 h after i.v. neuraminidase or PBS treatment. Antibody to CD41 was used to detect and quantify platelets in whole blood. In these studies mice were treated with either 5 U/kg of *Arthrobacter urefaciens* neuraminidase or PBS control. Studies included between 12 and 24 age-matched adult mice of indicated genotypes. ***$P < 0.001$.

a rapid rate of AMR-dependent platelet clearance after neuraminidase treatment, whereas platelet glycoproteins other than Gp1bα can also serve as AMR ligands.

Intravenous neuraminidase treatment was investigated as a means to reduce coagulopathy and enhance host survival during *SPN* sepsis. At lethal doses of *SPN*, animals receiving the PBS

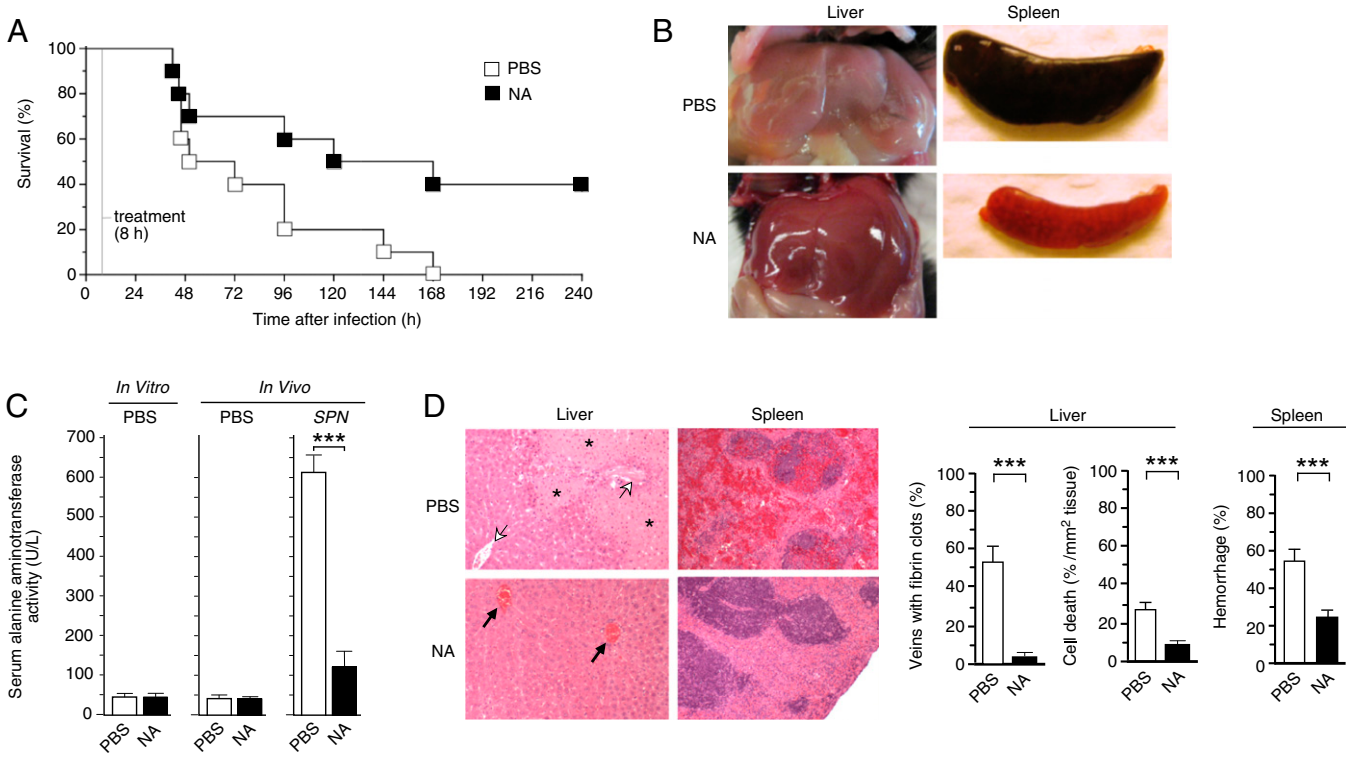

Fig. 2. Effects of intravenous neuraminidase treatment on coagulopathy, organ damage, and host survival in *SPN* sepsis. (*A*) WT mice were infected by i.p. injection of 10^4 cfu of *SPN* isolate D39, and survival was followed over time among cohorts receiving either *AUS* neuraminidase (NA) (5 U/kg) or PBS at 8 h after infection. More than 40 mice receiving each treatment were analyzed from multiple independent experiments. (*B*) Representative macroscopic views of liver and spleen 48 h after *SPN* infection. (*C*) Serum levels of alanine aminotransferase activity. (*D*) Histopathological analyses of liver and spleen tissue 48 h after infection exhibited fibrin thrombi and empty vessels (open arrows) indicative of thromboembolic occlusions. Functioning blood vessels containing red blood cells are also denoted (closed arrows). Pyknotic bodies indicating cell death are marked (asterisks). Fibrin clots, pyknotic bodies, and splenic hemorrhage were quantified. Studies in *B*–*D* compared 12–24 age-matched adult mice of indicated genotypes. ***$P < 0.001$.

sham treatment succumbed as expected. In contrast, half of the animals receiving a single treatment of i.v. neuraminidase survived (Fig. 2*A*). Neuraminidase treatment did not modify basic blood chemistry parameters during sepsis (Table S2). Host protection conferred by neuraminidase was closely associated with reduced histopathological evidence of injury to liver and spleen tissues, lower serum alanine aminotransferase levels (a marker of hepatocyte injury), and significant reductions in the frequency of fibrin clots, thromboembolic occlusions, hepatocyte pyknosis, and splenic hemorrhage (Fig. 2 *B–D*). The timing of neuraminidase administration after post-i.p. *SPN* infection was important in achieving a therapeutic response (Fig. S5).

The role of the AMR in host protection induced by neuraminidase was investigated among mice lacking the Asgr1 or Asgr2 component of the AMR. Both Asgr1 and Asgr2 were essential for the therapeutic effect of i.v. neuraminidase administration. At identical and lethal *SPN* challenge doses, neuraminidase treatment of animals lacking either Asgr1 or Asgr2 failed to mitigate disease, and all succumbed to sepsis, whereas at the same time ~50% of WT cohorts that received neuraminidase survived (Fig. 3*A*). Neuraminidase treatment of AMR-deficient mice did not alter various blood chemistry components compared with WT cohorts (Table S2). In contrast, alanine aminotransferase levels in the sera were markedly elevated in AMR deficiency, beyond that of WT counterparts, and remained significantly higher after neuraminidase treatment (Fig. 3*B*). Liver and splenic tissue damage in AMR deficiency were only moderately improved by neuraminidase treatment, judged by frequencies of fibrin clots, liver cell death, and splenic hemorrhage compared with WT animals (Fig. 3 *C* and *D*). The AMR is therefore required for host protection induced by i.v. neuraminidase treatment. This protection is associated with the clearance from circulation of desialylated blood components including platelets that would otherwise participate in the development of disseminated intravascular coagulation.

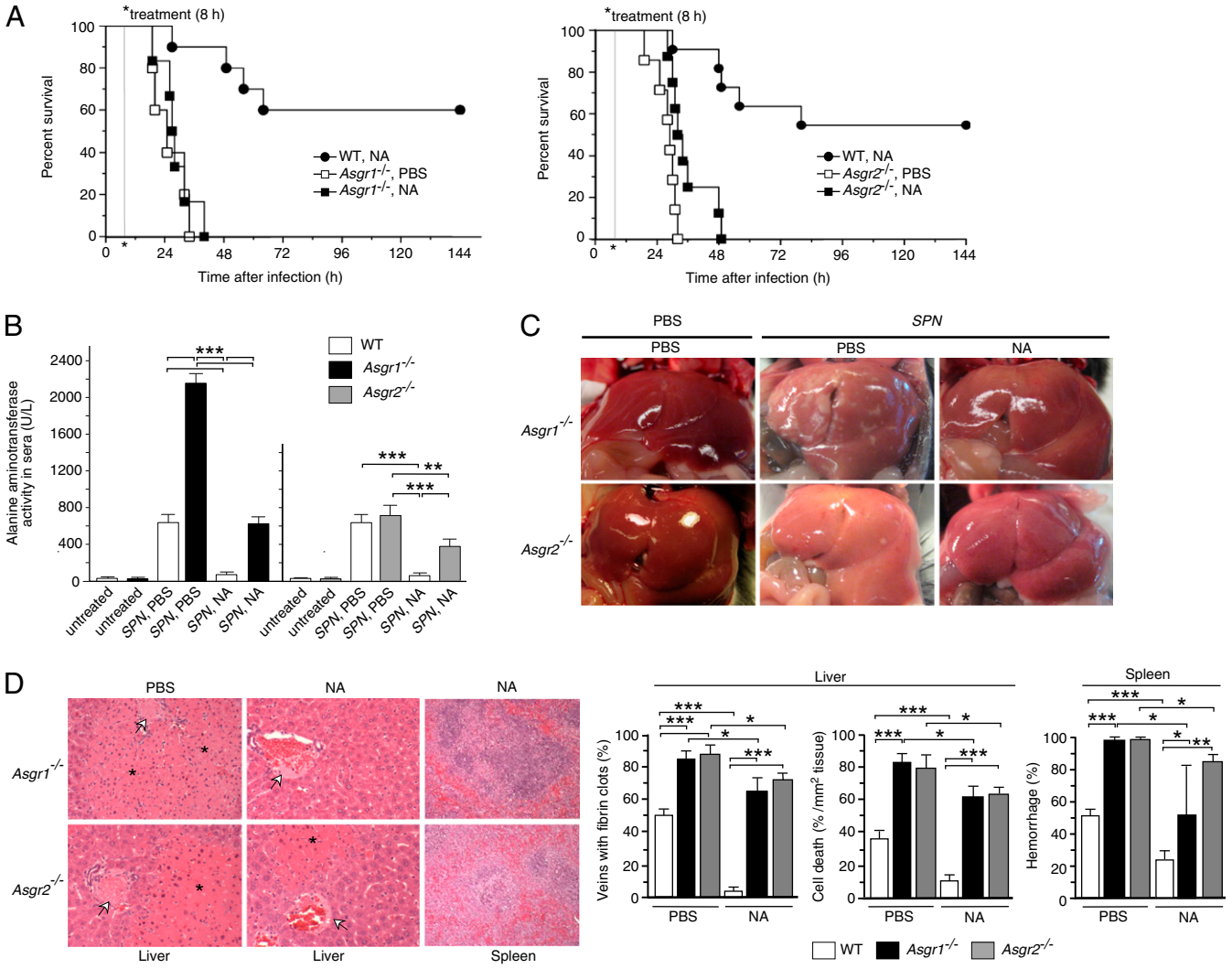

Fig. 3. AMR function in host protection after neuraminidase treatment during *SPN* sepsis. (*A*) Survival among cohorts of mice lacking either the Asgr1 or Asgr2 component of the AMR in the presence or absence of neuraminidase (NA) or PBS delivered by i.v. injection 8 h after i.p. injection of *SPN* isolate D39 (10^4 cfu). Each cohort of mice received either *AUS* neuraminidase (5 U/kg) or PBS at 8 h after infection. More than 40 mice of each genotype receiving the indicated treatments from multiple independent experiments were analyzed. (*B*) Serum levels of alanine aminotransferase activity at 48 h. (*C*) Representative macroscopic views of the liver and spleen 48 h after *SPN* infection. (*D*) Histopathological analyses of liver and spleen tissue 48 h after infection indicated fibrin deposition and empty blood vessels (open arrows). Pyknotic bodies indicating cell death are marked (asterisks). Fibrin clots, pyknotic bodies, and splenic hemorrhage were quantified. At least 12 age-matched mice of each genotype were analyzed in *B–D* from multiple independent experiments. ***$P < 0.001$, **$P < 0.01$, *$P < 0.05$.

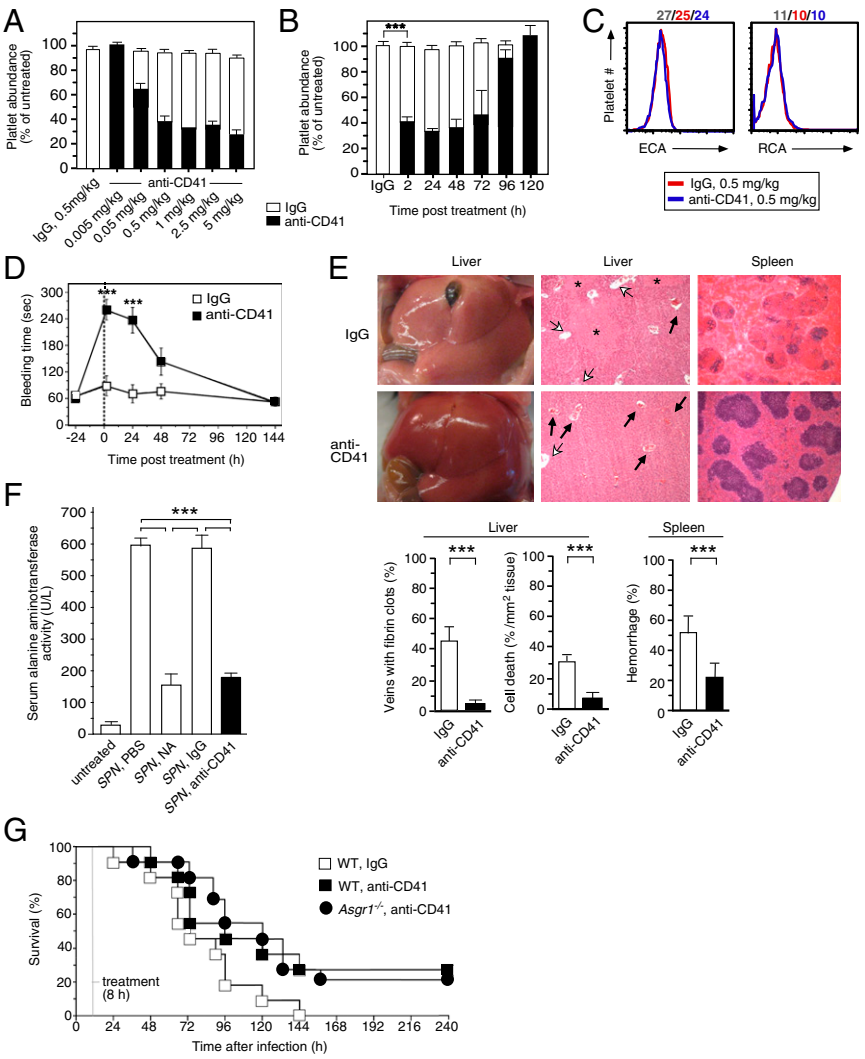

Fig. 4. Coagulopathy and host protection after anti-CD41 treatment and platelet depletion during *SPN* sepsis. (*A*) Platelet abundance in circulation 2 h after i.v. injection of anti-CD41 antibody or polyclonal IgG at indicated doses. (*B*) Platelet abundance in circulation at indicated times after a single i.v. injection (0.5 mg/kg) of either anti-CD41 or IgG. (*C*) ECA and RCA-I lectin binding at the platelet surface 2 h after i.v. injection (0.5 mg/kg) of either anti-CD41 or IgG. (*D*) Bleeding times after i.v. injection (0.5 mg/kg) of either anti-CD41 or IgG. (*E*) Representative macroscopic and histopathologic views of liver and spleen 48 h after *SPN* infection. Fibrin deposition and empty blood vessels are marked (open arrows). Blood vessels containing red blood cells are also denoted (closed arrows). Areas of pyknotic bodies indicating cell death are marked (asterisks). Fibrin clots, pyknotic bodies, and splenic hemorrhage were quantified. (*F*) Serum alanine aminotransferase activity. (*G*) Survival among mice receiving 0.5 mg/kg of either anti-CD41 or IgG 8 h after i.p. injection of *SPN* isolate D39 (10^4 cfu). At least 12 age-matched mice of each genotype were analyzed in *B*–*D* from multiple independent experiments. In *G*, more than 40 mice of each genotype receiving each treatment were analyzed in multiple independent experiments. Findings shown are representative of results obtained using anti-CD41 and IgG in either WT or AMR-deficient mice. ***$P < 0.001$.

The therapeutic impact of inducing a moderate thrombocytopenia was tested using an antibody-mediated (AMR-independent) platelet elimination strategy. Intravenous administration of antibody to the platelet-selective integrinα2β (CD41) rapidly induced a moderate thrombocytopenia and increased bleeding times in the absence of platelet desialylation, with a response closely paralleling neuraminidase treatment (Fig. 4 *A*–*D*). No changes in basic blood chemistry were observed after i.v. administration of anti-CD41 or IgG (Table S3). Analyses of liver and spleen tissues revealed that anti-CD41 treatment reduced vascular occlusions, fibrin clots, liver cell death, splenic hemorrhage, and alanine aminotransferase levels (Fig. 4 *E* and *F*). Platelet reduction by anti-CD41 treatment further improved survival frequencies at *SPN* challenge doses that killed all cohorts receiving the IgG sham treatment (Fig. 4*G*). As predicted, anti-CD41 antibody treatment of either WT or AMR-deficient mice produced similar results. These findings indicate that the intrinsic host protection provided by the AMR after i.v. neuraminidase administration is primarily achieved by the rapid induction of a moderate thrombocytopenia.

Comparing treatments and outcomes indicated that neuraminidase activation of the AMR achieved a somewhat greater protective measure than did anti-CD41 antibody. We found that i.v. neuraminidase treatment resulted in additional changes that primarily serve to lessen thrombosis. Neuraminidase increased activated partial thromboplastin time (aPTT)—a critical coagulation parameter, in both mice and human plasma (Fig. 5 *A* and *B*). The same anticoagulation effect was observed in AMR deficiency (Fig. 5*C*). No change from normal coagulation times occurred after anti-CD41 antibody treatment (Fig. 5*D*). Individual blood coagulation factor analyses after neuraminidase treatment revealed significant decreases in the abundance and activity of prothrombotic components, including von Willebrand factor and factors II, V, VIII, X, and XI (Fig. 6). These glycoproteins contribute to aPTT, and their decreased abundance and activity explain the increase in coagulation time. Decreases were also observed in antithrombotic components antithrombin and α2-antiplasmin, but they were of minor impact by comparison and would not overcome the induction of a hypocoagulative state caused by the combined reductions measured in prothrombotic factors. Other coagulation factors were unchanged by neuraminidase treatment, including factors I, VII, IX, and XII, plasminogen, fibrinogen, protein C, and protein S (Fig. S6). Absence of altered coagulation factor abundance and activity did not however indicate the absence of glycoprotein desialylation. Neuraminidase doses that reduced platelet levels in circulation similar to that observed after *SPN* infection also diminished sialic acid abundance on all glycoproteins analyzed, including those that were unaltered, indicating selectivity of the AMR for a subset of endogenous ligands in conferring host protection in pneumococcal

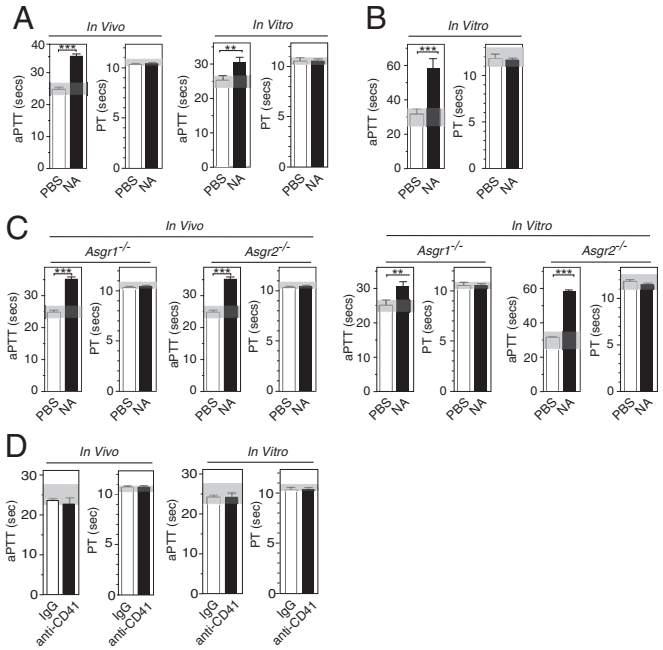

Fig. 5. (*A–D*) Treatment with neuraminidase (NA), but not anti-CD41 antibody, induces a hypocoagulative state in blood plasma. aPTT and partial thrombin (PT) time were determined in plasma after either in vivo or in vitro treatments with neuraminidase or anti-CD41 in parallel comparisons with PBS or IgG control treatments.

sepsis (6) (Fig. 7). Endogenous glycoproteins modulated by the AMR in the physiological context of pneumococcal sepsis include those with the largest numbers of potential *N*-glycosylation sites encoded in their primary peptide sequences (Table S4).

Discussion

The protective role of the host AMR is activated in response to increased neuraminidase activity in the bloodstream during sepsis. This is achieved in large part by neuraminidase-dependent unmasking of cryptic AMR ligands existing on platelets and a subset of prothrombotic blood coagulation factors. The endocytic AMR reduces the abundance of these desialylated prothrombotic components in producing a hypocoagulative state that lessens the potential for the onset of disseminated intravascular coagulation. Platelets and prothrombotic blood coagulation factors can play harmful roles in sepsis when they fuel pathogen-driven coagulopathy that results in thromboembolic tissue damage, often with a fatal outcome. Aberrations in platelet activity may further complicate sepsis by binding and disseminating bacteria throughout the bloodstream (16, 17) or by contributing to granzyme B-mediated killing of splenocytes (18). Regulation of glycoprotein homeostasis by the AMR has been imperceptible to multiple studies of genomic variation and transcriptional outputs, reflecting posttranslational and enzymatic processes that modulate metabolism and which are increasingly linked to the origins of common diseases and syndromes (19–22).

Endogenous glycoproteins bearing AMR ligands have been difficult to identify. Previous studies have included exogenously administered glycoproteins of multiple species often derived from heterologous cell expression systems and were used in isolation at various concentrations in circulation. The potential for ligand selectivity of the homomeric and heteromeric AMR complex in determining the relative binding and clearance rates among endogenous glycoproteins also remains to be fully studied. Given these complications, it has not been possible to identify and compare endogenous AMR ligands produced in a physiological context, as in the course of sepsis. In comparisons among multiple glycoproteins, we find that those modulated by the AMR and neuraminidase activity have the largest number of *N*-glycan sequons in their peptide sequences. Not all such sequons are necessarily modified with *N*-glycans; nevertheless, these findings suggest an evolutionary mechanism that may render a protein responsive to AMR clearance and further provides an experimental framework to determine structural features of endogenous AMR ligands that may involve glycan density in combination with glycoprotein sequence and structure.

AMR function protects a large fraction of septic animals from excessive tissue damage and death and appears to be required for host survival of severe sepsis caused by *SPN*. This *SPN* pathogen–host interaction is likely to have been a focus of millions of years of

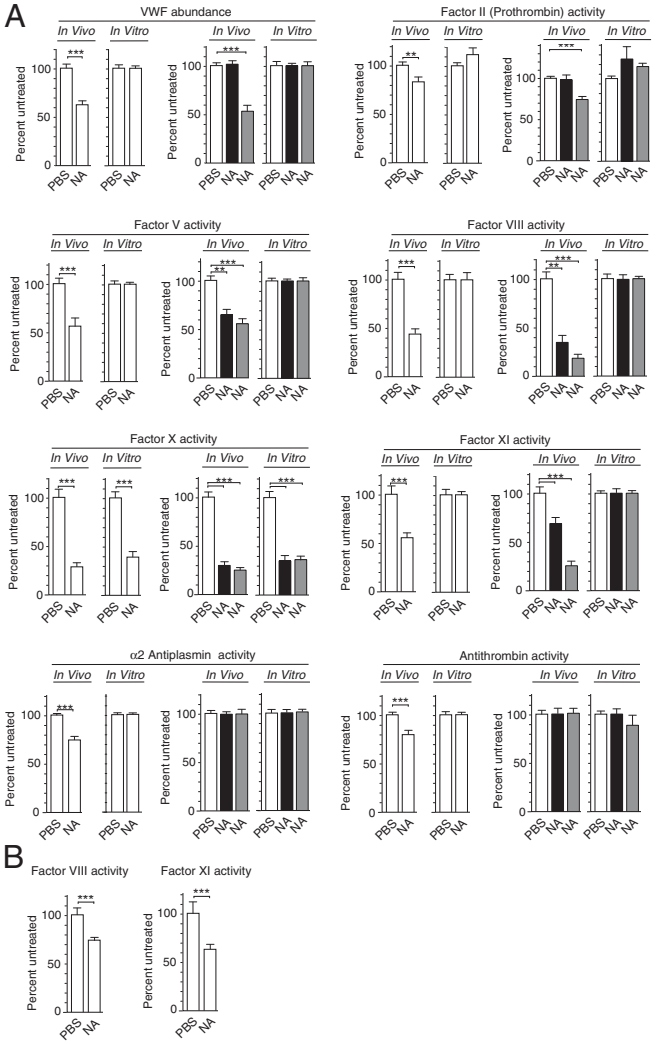

Fig. 6. Blood coagulation factor abundance or activity after (*A*) i.v. neuraminidase (NA) treatment in the presence or absence of AMR function in mice, and (*B*) in vitro neuraminidase treatment of human blood plasma. Wild-type or AMR-deficient mice were bled 2 h after i.v. treatment with either *AUS* NA (5 U/kg) or PBS. Plasma was isolated for measurements of the abundance or activity of specific blood coagulation factors, as previously described (24, 25). Measurements of glycoprotein abundance were obtained with anti-factor antibodies. Factor-specific enzyme activities were measured where indicated.

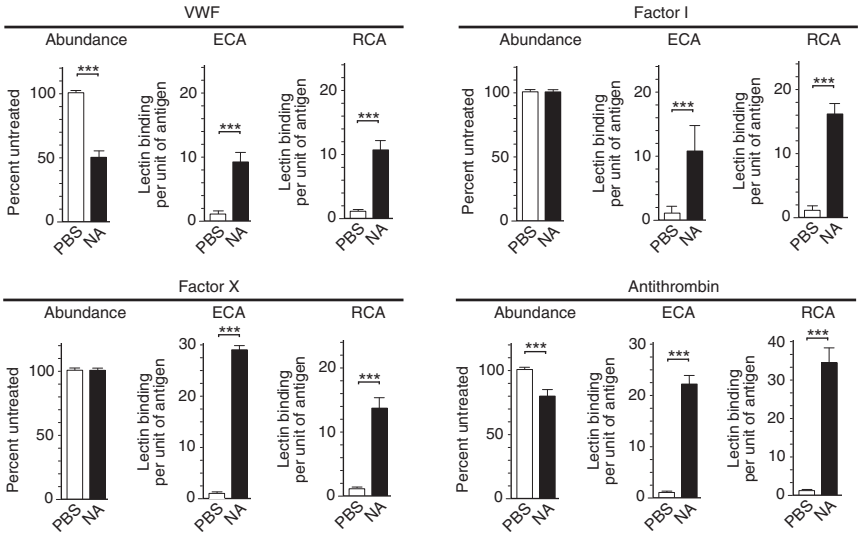

Fig. 7. Blood coagulation factor abundance and desialylation after i.v. neuraminidase (NA) treatment. Coagulation factor protein abundance measured by antibodies was further analyzed by ECA and RCA-I lectins to detect exposed galactose following i.v. treatment with either *AUS* NA (5 U/kg) or PBS. Ratios of exposed galactose per unit of protein antigen were calculated as indicated and as previously described (25).

evolution, providing a selective pressure favoring the endocytic AMR response to counteract pathogen perturbation of the host coagulation system. The AMR is, however, unable to rescue all infected animals owing to multiple pathogenic processes that are ongoing, including cytokine storm that can lead to lethality (23). When the AMR response is inadequate and as pathogen load increases, thrombosis continues, and platelets may be further consumed to less than 10% of normal levels in fulminant disseminated intravascular coagulation when hemorrhage itself becomes life threatening. It will be of interest to determine whether i.v. neuraminidase treatment is similarly therapeutic in sepsis caused by pathogens that lack an encoded neuraminidase. The finding that the "natural" process of AMR activation in pneumococcal sepsis is not optimal and can be improved upon reflects a biological response that has evolved to preserve species if not all individuals. Such protective mechanisms may be required for species survival, but may rarely if ever become optimized by natural selection. The targeted i.v. administration of neuraminidase during sepsis merits further exploration as a method to rapidly activate and augment the life-protective function of the host AMR.

Materials and Methods

Detailed methods, including descriptions of all reagents, are included in *SI Materials and Methods*. Data are presented as means ± SEM unless otherwise indicated. We used the Student unpaired *t* test, as well as Kaplan-Meier analyses of survival curves, with Prism software (GraphPad). Multiple-analyte sera data were compared by two-way ANOVA and *t* tests. *P* values of less than 0.05 were considered significant. Statistical significance is presented throughout as $***P < 0.001$, $**P < 0.01$, or $*P < 0.05$.

ACKNOWLEDGMENTS. This research was funded by National Institutes of Health Grant GM100192 (to J.D.M.).

1. Stearns-Kurosawa DJ, Osuchowski MF, Valentine C, Kurosawa S, Remick DG (2011) The pathogenesis of sepsis. *Annu Rev Pathol* 6:19–48.
2. Levi M, Schultz M, van der Poll T (2010) Sepsis and thrombosis. *Semin Thromb Hemost* 36:367–377.
3. Marshall JC (2001) Inflammation, coagulopathy, and the pathogenesis of multiple organ dysfunction syndrome. *Crit Care Med* 29(7, Suppl):S99–S106.
4. Giamarellos-Bourboulis EJ (2013) The failure of biologics in sepsis: Where do we stand? *Int J Antimicrob Agents* 42(Suppl):S45–S47.
5. Angus DC (2011) The search for effective therapy for sepsis: Back to the drawing board? *JAMA* 306(23):2614–2615.
6. Grewal PK, et al. (2008) The Ashwell receptor mitigates the lethal coagulopathy of sepsis. *Nat Med* 14(6):648–655.
7. Ashwell G, Morell AG (1974) The role of surface carbohydrates in the hepatic recognition and transport of circulating glycoproteins. *Adv Enzymol Relat Areas Mol Biol* 41(0):99–128.
8. Varki A, Gagneux P (2012) Multifarious roles of sialic acids in immunity. *Ann N Y Acad Sci* 1253:16–36.
9. Ohtsubo K, Marth JD (2006) Glycosylation in cellular mechanisms of health and disease. *Cell* 126(5):855–867.
10. Roggentin P, Schauer R, Hoyer LL, Vimr ER (1993) The sialidase superfamily and its spread by horizontal gene transfer. *Mol Microbiol* 9(5):915–921.
11. Tong HH, Liu X, Chen Y, James M, Demaria T (2002) Effect of neuraminidase on receptor-mediated adherence of *Streptococcus pneumoniae* to chinchilla tracheal epithelium. *Acta Otolaryngol* 122(4):413–419.
12. King SJ, Hippe KR, Weiser JN (2006) Deglycosylation of human glycoconjugates by the sequential activities of exoglycosidases expressed by *Streptococcus pneumoniae*. *Mol Microbiol* 59(3):961–974.
13. Manco S, et al. (2006) Pneumococcal neuraminidases A and B both have essential roles during infection of the respiratory tract and sepsis. *Infect Immun* 74(7):4014–4020.
14. Chang YC, Uchiyama S, Varki A, Nizet V (2012) Leukocyte inflammatory responses provoked by pneumococcal sialidase. *MBio*, 10.1128/mBio.00220-11.
15. Sørensen AL, et al. (2009) Role of sialic acid for platelet life span: Exposure of beta-galactose results in the rapid clearance of platelets from the circulation by asialoglycoprotein receptor-expressing liver macrophages and hepatocytes. *Blood* 114(8):1645–1654.
16. Sullam PM, Payan DG, Dazin PF, Valone FH (1990) Binding of viridans group streptococci to human platelets: A quantitative analysis. *Infect Immun* 58(11):3802–3806.
17. Kahn F, Hurley S, Shannon O (2013) Platelets promote bacterial dissemination in a mouse model of streptococcal sepsis. *Microbes Infect* 15(10-11):669–676.
18. Sharon M, et al. (2012) Platelets induce apoptosis during sepsis in a contact-dependent manner that is inhibited by GPIIb/IIIa blockade. *PLoS One* 7(7):e41549.
19. Marth JD (2008) A unified vision of the building blocks of life. *Nat Cell Biol* 10(9):1015–1016.
20. Ohtsubo K, Chen MZ, Olefsky JM, Marth JD (2011) Pathway to diabetes through attenuation of pancreatic beta cell glycosylation and glucose transport. *Nat Med* 17(9):1067–1075.
21. Langley RJ, et al. (2013) An integrated clinico-metabolomic model improves prediction of death in sepsis. *Sci Transl Med* 5(195):95ra95.
22. Wellen KE, Thompson CB (2012) A two-way street: Reciprocal regulation of metabolism and signalling. *Nat Rev Mol Cell Biol* 13(4):270–276.
23. Sriskandan S, Altmann DM (2008) The immunology of sepsis. *J Pathol* 214(2):211–223.
24. Wang Y, et al. (2001) Modeling human congenital disorder of glycosylation type IIa in the mouse: Conservation of asparagine-linked glycan-dependent functions in mammalian physiology and insights into disease pathogenesis. *Glycobiology* 11(12):1051–1070.
25. Ellies LG, et al. (2002) Sialyltransferase ST3Gal-IV operates as a dominant modifier of hemostasis by concealing asialoglycoprotein receptor ligands. *Proc Natl Acad Sci USA* 99(15):10042–10047.

Supporting Information

Grewal et al. 10.1073/pnas.1313905110

Materials and Methods

Animals. Animal use was limited to adult laboratory mice of the C57BL/6Hsd strain. All procedures were approved by Institutional Animal Care and Use Committees of the University of California Santa Barbara and the Sanford-Burnham Medical Research Institute. Mice were provided sterile pellet food and water ad libitum. Littermates and related cohorts aged 8–16 wk were used for experimentation. Mice lacking a functional gene encoding GPIbα (1) were kindly provided by Zaverio Ruggeri (The Scripps Research Institute, La Jolla, CA). Mice bearing null mutations in the genes encoding *Asgr1* or *Asgr2* have been previously described (2, 3). All alleles were maintained through at least eight generations of meiotic recombination in the C57BL/6NHsd background. All animals were provided sterile pellet food and water ad libitum. Littermates and related cohorts aged 8–16 wk were used for experimentation.

Human Subjects. The Institutional Review Board of the Cottage Health System approved experiments to acquire anonymous human blood samples for analysis upon informed consent of healthy volunteers.

Reagents. Chemicals, biologics, and other reagents used included *N*-hydroxysuccinimidobiotin (Pierce), paraformaldehyde (Electron Microscopy Sciences), biotin and FITC-conjugated lectins including *Erythrina cristagalli* lectin (ECA) and *Ricinus communis*-1 agglutinin (RCA-I) (Vector Laboratories), CellTracker Orange (Molecular Probes), alkaline phosphatase (Sigma), streptavidin-alkaline phosphatase (BD Pharmingen), Todd-Hewitt broth (Teknova), RBC lysis buffer (eBioscience), BSA (Jackson Immunoresearch), serum-separator, and EDTA-Vacutainer tubes (Becton Dickinson). Enzymes used were *Clostridium histolyticum* collagenase (Sigma-Aldrich), *Streptococcus pneumoniae* (*SPN*) NanA neuraminidase (Seikagaku/Northstar Bioproducts), *Vibrio cholerae* (*VC*) neuraminidase (Roche Applied Science), or *Arthrobacter ureafaciens* (*AUS*) neuraminidase (EY Laboratories). Antibodies included FITC or DyLight649-conjugated rat antibodies that bind to CD42a (GPIX, clone Xia.B4), CD42b (GP1bα, clone Xia.G5), and CD42c (GPIbβ, clone Xia.C3) (Emfret Analytics), FITC- or Phycoerythrin (PE)-conjugated antibodies to CD41 (MWReg30) and a polyclonal IgG control (BD Pharmingen), FITC- or APC-conjugated anti-CD61 (2C9.G3), anti-TER119, and all isotype controls (eBiosciences), von Willebrand Factor (DAKO), antithrombin, coagulation factors I, II, and X (Hematologic Technologies), and PE-conjugated anti-Gr1 (clone RB6-8C5) and anti-CD3 (2C11) (eBioscience).

Bleeding Times. Mice were anesthetized and restricted horizontally. The tail was severed 2 mm from the tip (or additional 1 mm for subsequent time points) with a razor blade and immersed vertically 1 cm below the surface of 37 °C saline. Time until bleeding stopped was recorded. Cauterization was not required.

Coagulation and Hematology. Blood used in coagulation assays was collected by cardiac puncture. Citrated platelet-poor plasma was prepared from citrated blood by centrifugation at 22 °C. Plasma samples were aliquoted and frozen at −80 °C within 4 h of blood collection. Hematology assessment, blood coagulation time assays, platelet counts, and blood coagulation factor assays were performed as previously described (4–6). Platelets were identified using flow cytometry with either anti-CD41 or anti-CD61 antibodies.

Blood Chemistry and Cytokine Measurements. Blood was collected from the retroorbital sinus while the mouse was kept under general (inhalant) anesthesia. Blood was collected into Microtainer Serum Separator Tubes (BD) with no anticoagulant and allowed to clot for 30 min at room temperature. Sera collected after centrifugation at 13,000 rpm for 10 min. For blood chemistry, a VetScan Comprehensive Diagnostic Profile reagent rotor was used with the VetScan Chemistry Analyzer according to the manufacturers' instructions.

Neuraminidase and Anti-CD41 Treatment. For in vitro treatment, isolated whole blood was incubated with neuraminidase doses as indicated in the text, ranging from 0.001 to 0.3 U/mL for 2 h at 37 °C before analysis. For in vivo treatment, neuraminidase or antibody was i.v. injected into the retroorbital sinus or the tail vein. Neuraminidase doses ranging from 0.25 to 50 U/kg in 100 μL diluted with PBS were i.v. injected (via retroorbital sinus). Anti-CD41 or polyclonal IgG control (0.5 mg/kg) were diluted up to 100 μL in PBS and delivered i.v. into the retroorbital plexus. Serial samples were taken by retroorbital sinus bleeds after injection. Each mouse was bled up to 3 time points for analyses of coagulation factor levels or activity.

Mouse Platelet Isolation, Survival, and Fate. Whole blood was incubated in vitro with indicated neuraminidase at specified dose for 2 h at 37 °C. For the final 30 min, CellTracker red was added to 2- μM final concentration. Platelet-rich plasma was prepared by centrifugation at 268 × *g* for 8 min. Platelets were separated from platelet-rich plasma by centrifugation at 834 × *g* for 5 min and washed twice in Tyrode's buffer (137 mmol/L NaCl, 2.8 mmol/L KCl, 1 mmol/L $MgCl_2$, and 10 mmol/L Hepes, pH 7.4) to remove excess CellTracker dye. Platelet-rich plasma from donor mice were used in in vitro experiments or infused into recipient mice of indicated genotypes via retroorbital sinus in a maximum volume of 200 μL. Blood samples were obtained at indicated time points to evaluate circulatory half-life of donor platelets in recipient mice by flow cytometry. Platelets were identified by forward- and side-scatter profiles and confirmed by anti-CD41 antibody binding. The relative proportion of CellTracker-loaded infused donor platelets remaining in circulation (visible in phycoerythrin detection channel) was calculated as a percentage of that measured at the first time point collected 1 to 2 min after transfusion.

***SPN* Infection.** Wild-type (*SPN*) serotype 2 isolate D39 was used throughout the study as previously described (3). All bacterial infections were administered by i.p. injection at cfu doses indicated.

Histology. Tissues were fixed in 10% (vol/vol) buffered formalin, trimmed, processed, embedded in paraffin, sectioned at a width of 5 μm, histochemically stained, and visualized by light microscopy at magnifications indicated and as previously described (3).

1. Ware J, Russell S, Ruggeri ZM (2000) Generation and rescue of a murine model of platelet dysfunction: The Bernard-Soulier syndrome. *Proc Natl Acad Sci USA* 97(6):2803–2808.
2. Soukharev S, Miller JL, Sauer B (1999) Segmental genomic replacement in embryonic stem cells by double lox targeting. *Nucleic Acids Res* 27(18):e21.
3. Ishibashi S, Hammer RE, Herz J (1994) Asialoglycoprotein receptor deficiency in mice lacking the minor receptor subunit. *J Biol Chem* 269(45):27803–27806.
4. Grewal PK, et al. (2008) The Ashwell receptor mitigates the lethal coagulopathy of sepsis. *Nat Med* 14(6):648–655.

5. Wang Y, et al. (2001) Modeling human congenital disorder of glycosylation type IIa in the mouse: Conservation of asparagine-linked glycan-dependent functions in mammalian physiology and insights into disease pathogenesis. *Glycobiology* 11(12): 1051–1070.

6. Ellies LG, et al. (2002) Sialyltransferase ST3Gal-IV operates as a dominant modifier of hemostasis by concealing asialoglycoprotein receptor ligands. *Proc Natl Acad Sci USA* 99(15):10042–10047.

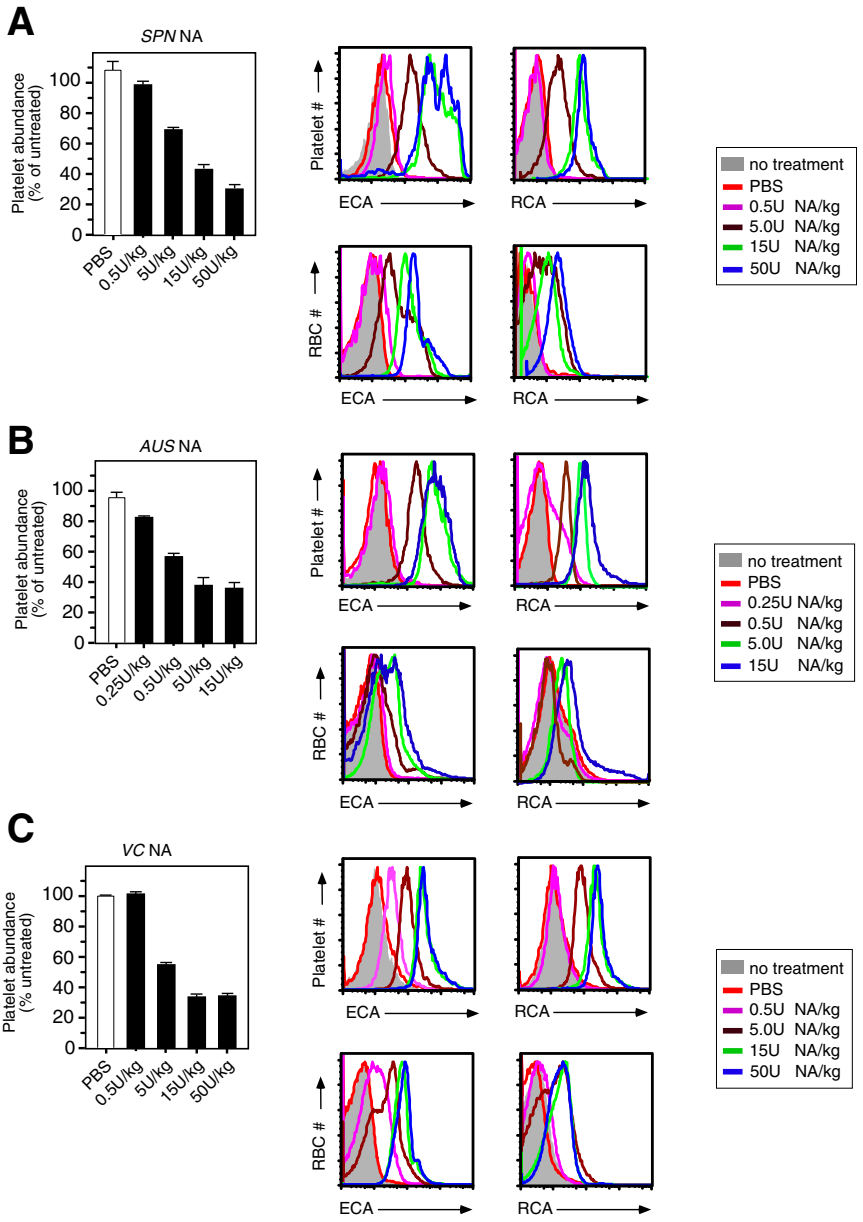

Fig. S1. Dose–response of microbial neuraminidases in platelet desialylation and the induction of thrombocytopenia. Circulating platelet sialylation and abundance in WT mice were measured by flow cytometry 2 h after i.v. administration of indicated doses of neuraminidase (NA) obtained from (*A*) *SPN*, (*B*) *AUS*, and (*C*) *VC*. Platelets were identified with anti-CD41 antibody. Red blood cells were identified with Ter-119 antibody. Exposure of galactose after desialylation was simultaneously determined with ECA and RCA-I lectins.

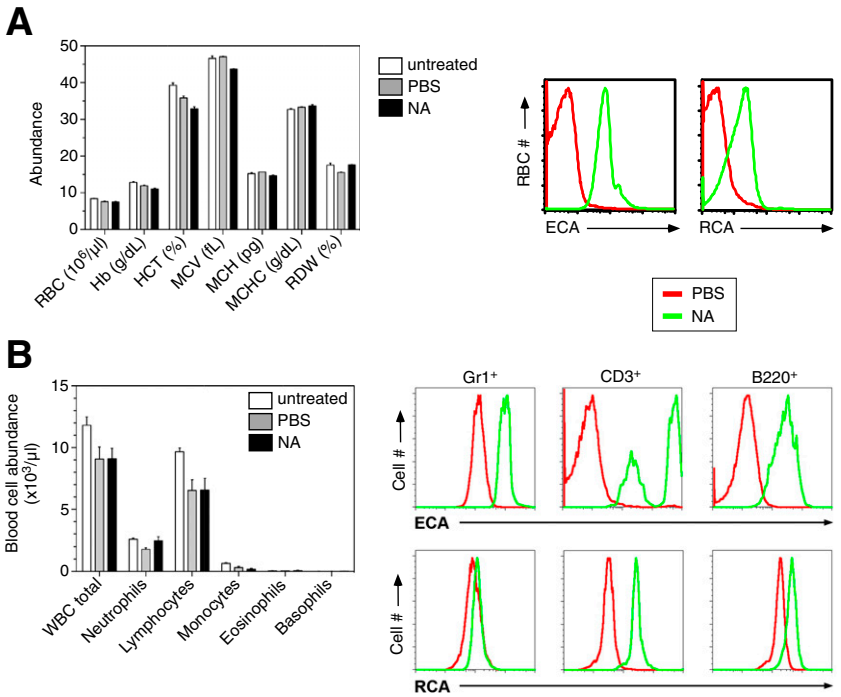

Fig. S2. Hematological measurements after i.v. neuraminidase treatment. Wild-type mice were bled 2 h after i.v. treatment with neuraminidase (NA) or PBS before measuring (*A*) red blood cell parameters and (*B*) nucleated blood cell measurements. Desialylation of blood cells representing neutrophils ($Gr1^+$), T cells ($CD3^+$), and B cells ($B220^+$) were determined by flow cytometry with measurements of ECA and RCA-I lectin binding. Similar results were observed at 24 h after treatment. HCT, hematocrit; MCH, mean corpuscular hemoglobin; MCHC, mean corpuscular hemoglobin concentration; MCV, mean corpuscular volume; RDW, red blood cell distribution width.

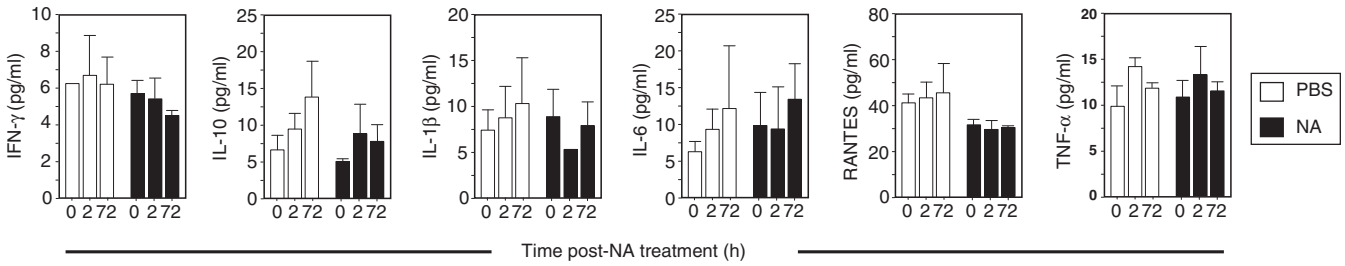

Fig. S3. Inflammation marker abundance in the blood after neuraminidase (NA) treatment. Abundance of indicated cytokines in blood sera determined using ELISA at multiple time points after i.v. administration of PBS or neuraminidase to WT mice. RANTES (regulated on activation, normal T cell expressed and secreted) is also Chemokine ligand 5 (CCL5).

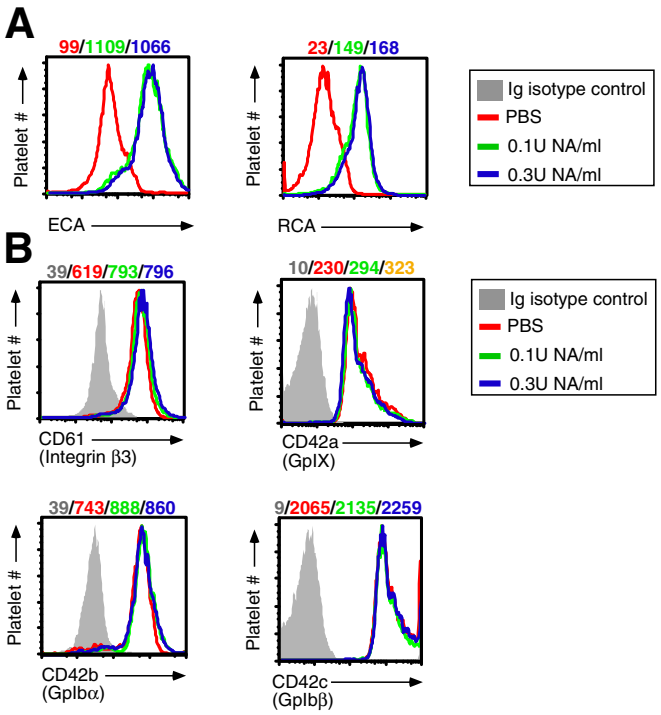

Fig. S4. Desialylation and glycoprotein abundance at the surface of platelets after neuraminidase (NA) treatment. (*A*) Platelet desialylation and (*B*) platelet glycoprotein abundance were measured in vitro 30 min after the addition of neuraminidase or PBS at the indicated dosages to isolated whole blood.

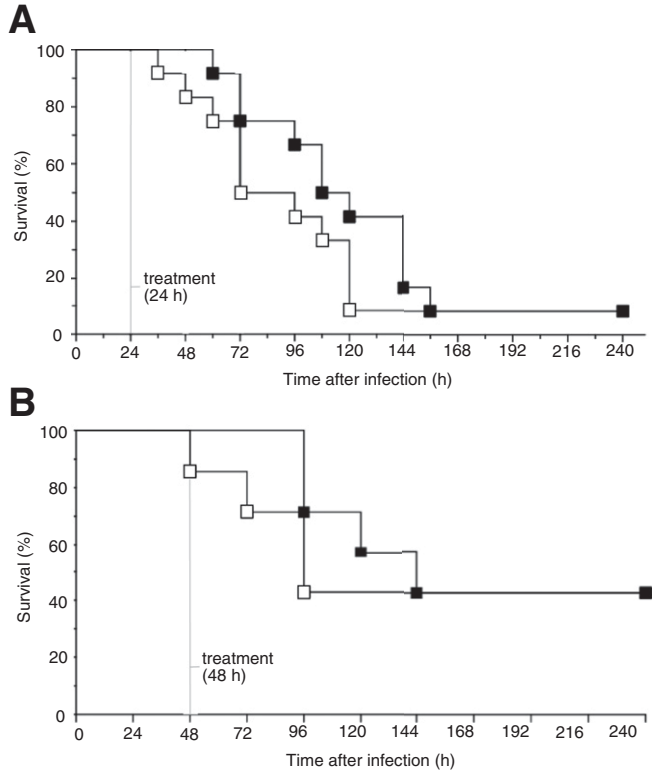

Fig. S5. Survival of mice administered i.v. neuraminidase at different times after *SPN* infection. (*A*) WT mice were infected with a lethal dose (2×10^5 cfu) of *SPN* by i.p. injection and were administered PBS or neuraminidase i.v. 24 h after infection. In parallel studies, (*B*) WT mice were infected with an LD_{50} dose (1×10^3 cfu) of *SPN* by i.p. injection and were administered PBS or neuraminidase i.v. 48 h after infection. White squares, PBS treatments; black squares, neuraminidase treatments.

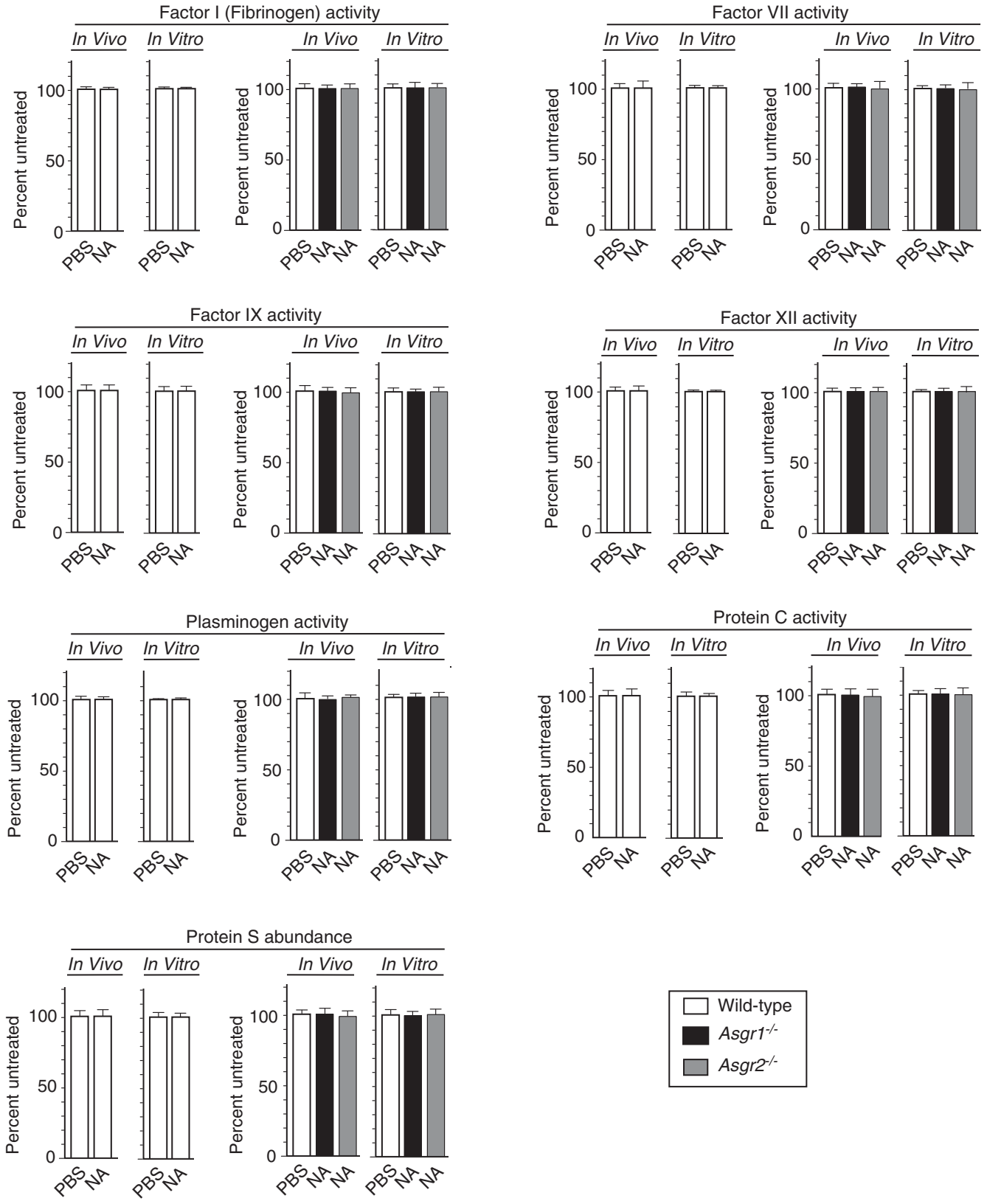

Fig. S6. Abundance or activity of blood coagulation factors by i.v. neuraminidase treatment. WT and Ashwell-Morell receptor (AMR)-deficient mice were bled 2 h after i.v. treatment with either neuraminidase (NA) or PBS. Plasma was isolated for measurements of blood coagulation factor abundance and activity as previously described (5, 6).

Table S1. Blood chemistry in WT mice after neuraminidase administration in vivo and in vitro

Analyte	In vitro PBS	In vitro NA	In vivo PBS	In vivo *SPN* NA	In vivo *AUS* NA	In vivo *VC* NA
Albumin (g/dL)	2.9 ± 0.3	2.9 ± 0.4	3.6 ± 0.2	4.2 ± 0	3.3 ± 0.1	3 ± 0.2
Alanine aminotransferase (U/L)	47.3 ± 11	48.5 ± 10.2	43.6 ± 9.5	33.5 ± 13	43.8 ± 3.5	39 ± 6.5
Amylase (U/L)	937 ± 64	921 ± 53	795.5 ± 135.3	791.5 ± 168.5	784.0 ± 145.5	850 ± 199
Total bilirubin (mg/dL)	0.2 ± 0	0.2 ± 0	0.2 ± 0.0	0.3 ± 0	0.2 ± 0.0	0.2 ± 0
Total nitrogen (mg/dL)	21 ± 1	20.3 ± 1.1	10.5 ± 2.1	24.5 ± 1	18.3 ± 6.8	15.5 ± 1.5
Calcium (mg/dL)	8.9 ± 0.1	8.7 ± 0.2	9.0 ± 0.1	9.1 ± 0	9.3 ± 0.1	9.56 ± 0.1
Phosphorus (mg/dL)	9 ± 0.4	11.2 ± 1.4	9.7 ± 0.5	8.2 ± 0.6	8.0 ± 1.4	7.8 ± 0.2
Creatinine (mg/dL)	0.2 ± 0	0.2 ± 0	0.2 ± 0	0.2 ± 0	0.2 ± 0.0	0.2 ± 0
Glucose (mg/dL)	191 ± 5	189.3 ± 2.6	169.5 ± 9	175.5 ± 9.5	179.0 ± 5.1	173 ± 2
Sodium (mmol/L)	151 ± 2	153 ± 0.6	151.5 ± 1.4	151 ± 1	151.1 ± 1.8	154.5 ± 0.5
Potassium (mmol/L)	4.7 ± 0.5	5.6 ± 0.5	5.2 ± 0.3	4.7 ± 0.5	5.7 ± 0.5	4.8 ± 0.2
Total protein (g/dL)	4.7 ± 0.2	4.6 ± 0.2	4.9 ± 0.2	5.1 ± 0.2	4.5 ± 0.1	4.6 ± 0.1
Globulin (g/dL)	1.7 ± 0.2	1.7 ± 0.2	1.5 ± 0.2	0.9 ± 0.2	1.6 ± 0.3	1.5 ± 0.1

In vivo analyses were accomplished among sera isolated 2 h after i.v. administeration of PBS or neuraminidase (NA). In vitro analyses were accomplished on sera prepared 30 min after addition of PBS or neuraminidase to isolated whole blood.

Table S2. Blood chemistry during *SPN* infection and NA treatment in WT and AMR-deficient (*Asgr1* or *Asgr2*) mice

Analyte	WT *PBS* *PBS*	WT *SPN* PBS	WT *SPN* NA	$Asgr1^{-/-}$ untreated	$Asgr1^{-/-}$ *SPN* PBS	$Asgr1^{-/-}$ *SPN* NA	$Asgr2^{-/-}$ untreated	$Asgr2^{-/-}$ *SPN* PBS	$Asgr2^{-/-}$ *SPN* NA
Albumin (g/dL)	3.7 ± 0.1	2.7 ± 0.2	1.5 ± 0.2	3.6 ± 0.2	3.2 ± 0.4	2.3 ± 0.2	3.6 ± 0.1	2.5 ± 0.2	2.0 ± 0.2
Amylase (U/L)	815 ± 57.2	1768 ± 331	2109 ± 459	739 ± 75.9	1128 ± 51	1367 ± 185	705 ± 49.3	1016 ± 170	1467 ± 309
Total bilirubin (mg/dL)	0.2 ± 0	0.2 ± 0.0	0.25 ± 0.02	0.2 ± 0	0.2 ± 0.0	0.25 ± 0.02	0.2 ± 0	0.3 ± 0.1	0.3 ± 0.04
Calcium (mg/dL)	9.0 ± 0.1	9.9 ± 0.2	8.0 ± 0.4	9.7 ± 0.3	9.0 ± 0.5	8.3 ± 0.4	9.4 ± 0.1	10.1 ± 0.1	8.5 ± 0.3
Phosphorus (mg/dL)	7.6 ± 0.5	7.6 ± 0.8	12.2 ± 1.7	9.7 ± 0.7	9.6 ± 0.4	15.6 ± 1.3	8.8 ± 0.4	9.3 ± 1.1	12.4 ± 2.6
Creatinine (mg/dL)	0.2 ± 0.01	0.2 ± 0.01	0.23 ± 0.02	0.2 ± 0	0.22 ± 0.02	0.28 ± 0.04	0.2 ± 0	0.2 ± 0	0.23 ± 0.03
Glucose (mg/dL)	156.9 ± 11.8	147.0 ± 2.6	167.0 ± 15.7	142.9 ± 11.9	144.7 ± 12.9	147.0 ± 14.2	163.0 ± 13	152.3 ± 6.7	146.5 ± 14.9
Sodium (mmol/L)	149.8 ± 1.1	152.3 ± 1.2	149.5 ± 0.7	154.4 ± 1.3	149.3 ± 1.2	152.7 ± 1.9	147.9 ± 1.2	145.0 ± 2.3	147.3 ± 2.3
Potassium (mmol/L)	5.0 ± 0.3	5.5 ± 0.3	5.7 ± 0.5	5.1 ± 0.1	5.4 ± 0.4	6.1 ± 0.6	5.2 ± 0.2	5.2 ± 0.2	4.9 ± 0.3
Total protein (g/dL)	4.7 ± 0.1	5.5 ± 0.1	3.6 ± 0.2	5.2 ± 0.3	5.1 ± 0.2	4.8 ± 0.2	4.9 ± 0.1	4.6 ± 0.3	4.2 ± 0.2
Globulin (g/dL)	1.2 ± 0.1	2.7 ± 0.2	2.0 ± 0.1	1.6 ± 0.1	2.8 ± 0.1	2.4 ± 0.2	1.3 ± 0.1	2.1 ± 0.3	2.3 ± 0.3

Measurements were completed on sera prepared from untreated or *SPN*-infected mice of the indicated genotypes 24 h after infection and 16 h after i.v. administration of PBS or neuraminidase (NA).

Table S3. Blood chemistry during *SPN* infection and antiplatelet antibody treatment

Analyte	$Asgr1^{-/-}$ untreated	$Asgr1^{-/-}$ *SPN* IgG	$Asgr1^{-/-}$ *SPN* anti-CD41	*Asgr-2*$^{-/-}$ untreated	$Asgr2^{-/-}$ *SPN* IgG	$Asgr2^{-/-}$ *SPN* anti-CD41
Albumin (g/dL)	3.6 ± 0.2	2.5 ± 0.3	2.2 ± 0.2	3.6 ± 0.1	2.6 ± 0.2	2.7 ± 0.2
Amylase (U/L)	739 ± 75.9	1012 ± 148	948 ± 111.8	705 ± 49.3	1528 ± 252	1071 ± 154.8
Total bilirubin (mg/dL)	0.2 ± 0	0.2 ± 0.0	0.23 ± 0	0.2 ± 0	0.5 ± 0.2	0.22 ± 0.02
Calcium (mg/dL)	9.7 ± 0.3	8.6 ± 0.7	9.9 ± 0.2	9.4 ± 0.1	9.2 ± 0.4	9.2 ± 0.3
Phosphorus (mg/dL)	9.7 ± 0.7	9.5 ± 0.8	10.1 ± 0.9	8.8 ± 0.4	12.3 ± 2.5	11.5 ± 2.3
Creatinine (mg/dL)	0.2 ± 0	0.23 ± 0.03	0.25 ± 0.1	0.2 ± 0	0.2 ± 0	0.24 ± 0.04
Glucose (mg/dL)	142.9 ± 11.9	138.3 ± 5.3	168.5 ± 25.4	163.0 ± 13	134.7 ± 16	149 ± 10.8
Sodium (mmol/L)	154.4 ± 1.3	152.3 ± 1.9	158 ± 2.3	147.9 ± 1.2	151.3 ± 1.9	146.8 ± 2.1
Potassium (mmol/L)	5.1 ± 0.1	5.6 ± 0.3	6.1 ± 0.4	5.2 ± 0.2	5.9 ± 0.5	5.8 ± 0.6
Total protein (g/dL)	5.2 ± 0.3	4.7 ± 0.3	5.0 ± 0.2	4.9 ± 0.1	4.6 ± 0.2	4.9 ± 0.2
Globulin (g/dL)	1.6 ± 0.1	2.5 ± 0.2	2.8 ± 0.1	1.3 ± 0.1	2.2 ± 0.3	2.3 ± 0.2

Measurements were completed on sera prepared from untreated or *SPN*-infected mice 24 h after infection and 16 h after i.v. treatment with anti-CD41 or polyclonal IgG antibodies.

Table S4. *N*-glycosylation consensus sites in human and mouse protein orthologs

	Homo sapiens			*Mus musculus*		
Glycoprotein	Total amino acids	No. of sites	*N*-site position	Total amino acids	No. of sites	*N*-site position
I (α-Fibrinogen)	866	3	419; 686; 831	789	2	609; 754
I (β-Fibrinogen)	491	1	**394**	481	1	**384**
I (γ-Fibrinogen)	453	1	**78**	436	1	**77**
II (Prothrombin)	622	4	**121; 143; 205; 416**	618	5	**122; 144; 207; 413;** 553
V	2,224	37	51; 55**; 239; 297; 382; 460;** 468**; 554;** 667; **741; 752; 760; 776;** 782; **821;** 938; 977; 1074; 1083; 1103; 1106; 1203; 1221; 1257; 1266; 1293; 1311; 1338; 1347; 1374; 1383; 1479; 1499; 1559; 1703; 2010; 2209	2183	26	176; **238; 296; 381; 459; 552; 740; 751; 759; 775; 820;** 841; 959; 972; 1038; 1049; 1058; 1067; 1088; 1438; 1459; 1460; 1519; 1663; 1811; 2168
VII	466	2	205; 382	446	2	186; 244
VIII	2,351	25	**60; 258; 601;** 776; 803; 847; 919; **962;** 982; **1020; 1024; 1074; 1085;** 1204; **1274; 1278; 1301; 1319;** 1403; 1431; 1461; 1531; 1704; 1829; 2137	2319	26	**61;** 233; **259;** 423; **601;** 880; **958;** 1015; **1022; 1026;** 1044; **1076; 1087;** 1136; 1161; 1192; 1255; 1268**; 1273; 1274; 1302; 1316;** 1340; 1378; 1797; 2105
IX	461	2	**203;** 213	471	4	36; **204;** 223; 316
X	488	2	**221;** 231	481	2	187; **218**
XI	625	5	**90; 126; 353; 450; 491**	624	6	**90; 126;** 297; **355; 449; 490**
XII	615	2	**249;** 433	597	4	**249;** 271; 324; 415
vWF	2,813	16	**99; 156;** 211**; 666; 857; 1231; 1515; 1574; 2223; 2290;** 2357**; 2400; 2546; 2585;** 2635; **2790**	2813	15	**99; 156; 666; 857;** 1005; **1231; 1515; 1574; 2223; 2290; 2400; 2546; 2585; 2790;** 2810
Antithrombin	464	4	**128; 167; 187; 224**	465	4	**129; 168; 188; 225**
Protein C	461	3	139; **290; 355**	460	3	214; **290; 354**
Protein S	676	3	**499; 509;** 530	675	2	**499; 509**
Plasminogen	810	1	**307**	812	2	136; **307**
α2 Antiplasmin	491	4	**126; 295; 309; 316**	491	4	**126; 295; 309; 316**

Numbers and positions of *N*-glycosylation consensus sites in each ortholog with site positions indicated relative to methionine at position 1. *N*-glycosylation consensus sites are defined as Asn-Xaa-Ser/Thr (NXS/T), where Xaa is any amino acid except proline. Numbers in bold indicate *N*-glycosylation sequons/positions conserved between human and mouse orthologs. Protein sequences were obtained from the UniProt Knowledgebase (www.uniprot.org) and analyzed using *NetNGlyc* (http://www.cbs.dtu.dk/).